

The single molecular precursor approach to metal telluride thin films: imino-bis(diisopropylphosphine tellurides) as examples

Jamie S. Ritch,^a Tristram Chivers,^{*a} Mohammad Afzaal^b and Paul O'Brien^{*b}

Received 20th April 2007

First published as an Advance Article on the web 27th June 2007

DOI: 10.1039/b605535b

Interest in metal telluride thin films as components in electronic devices has grown recently. This *tutorial review* describes the use of single-source precursors for the preparation of metal telluride materials by aerosol-assisted chemical vapour deposition (AACVD) and acquaints the reader with the basic techniques of materials characterization. The challenges in the design and synthesis of suitable precursors are discussed, focusing on metal complexes of the recently-developed imino-bis(diisopropylphosphine telluride) ligand. The generation of thin films and nanoplates of CdTe, Sb₂Te₃ and In₂Te₃ from these precursors are used as illustrative examples.

1 Introduction

Current interest in metal chalcogenides (sulfides, selenides or tellurides) stems, *inter alia*, from their unique optoelectronic, magneto-optic, thermoelectric and piezoelectric properties.¹ Potential applications of these semiconducting materials in devices such as solar cells (II–VI and III–VI),[†] infrared detectors (IV–VI) and room-temperature thermoelectric generators (V–VI) are under intense scrutiny. Modern technology often requires the growth of thin layers of different materials, one on top of another. The existing industrial process is known

as metal–organic vapour phase epitaxy (MOVPE) and was developed in the 1980s. It involves the transport of two precursors, often an organometallic compound and a volatile chalcogen source, under a hydrogen atmosphere to a chamber containing the heated wafer on which the semiconducting film is to be deposited. The obvious disadvantages of this process include: (a) the pyrophoric nature of precursors such as Me₃Ga or Me₂Cd and (b) the high toxicity of chalcogen sources such as H₂S, H₂Se and dialkyl tellurides. Another approach to the generation of binary and ternary semiconductors as thin films or nanocrystalline materials involves the use of single-source precursors (SSPs), *i.e.* compounds in which the desired metal and the chalcogen are contained in a single molecule.^{2,3}

In order to provide a well-defined focus for this *tutorial review*, the discussion will primarily be limited to recent work on metal tellurides as illustrative of the concepts and techniques involved in this route to compound semiconductors. The first part of the review will address the properties and

^aDept of Chemistry, University of Calgary, Calgary, AB, Canada T2N 1N4. E-mail: chivers@ucalgary.ca

^bThe School of Chemistry and The School of Materials, The University of Manchester, Oxford Road, Manchester, UK M13 9PL.

E-mail: paul.obrien@manchester.ac.uk; Fax: +44-161-2754616

[†]The designations II, III, IV *etc.*, generally accepted in the materials community, are used to describe compound semiconductors. Later in the article, the molecular compounds of the corresponding p-block elements are identified as group 12, 13, 14 *etc.*



Jamie S. Ritch

Jamie Ritch was born in Prince George, British Columbia, in 1983. He received his BSc (first class honours) degree in Chemistry from the University of Calgary in 2005. Currently he is in the PhD programme at the University of Calgary under the mentorship of Professor Tris Chivers. He is the recipient of an NSERC CGS-D postgraduate scholarship, an Alberta Ingenuity Incentive award, and an Honorary Izaak Walton Killam Memorial Scholarship from the University of

Calgary. His research interests are in the general area of main group chemistry with a focus on chalcogen compounds.

Tristram Chivers, a native of Bath, England, received his BSc, PhD and DSc degrees all from the University of Durham (UK). He



Tristram Chivers

joined the University of Calgary in 1969 and served as Head of the Chemistry Department from 1977 to 1982. He currently holds the titles of Faculty Professor and Professor Emeritus of Chemistry. His primary research interests are in the general area of main group element chemistry. He received the Alcan Lecture Award of the Canadian Society for Chemistry (CSC) in 1987, the E.W.R. Steacie Award from the CSC in 2001, and the Royal Society of Chemistry Award (UK) for Main-Group Element Chemistry in 1993. He was elected a Fellow of the Royal Society of Canada in 1991. He received an honorary DSc from the University of Oulu, Finland in 2006.

Table 1 Stoichiometries, structures and selected physical properties of some metal tellurides (E_{dir} = direct band gap, E_{ind} = indirect band gap, E_{opt} = optical band gap)⁷

Metal telluride	Structure	Lattice parameters/Å	Band gap/eV (T/K)
CdTe	Cubic	a 6.482	E_{dir} 1.49 (300)
ZnTe	Cubic	a 6.10	E_{dir} 2.28 (293)
HgTe ^a	Cubic	a 6.46	E_{dir} -0.141 (300)
β -GaTe	Monoclinic	a 17.44, b 10.464, c 4.077	E_{dir} 1.69 (295)
InTe	Tetragonal	a 8.454, c 7.152	Metallic as well as semiconducting
In ₄ Te ₃	Orthorhombic	a 15.630, b 12.756, c 4.441	E_{dir} 0.50 (300)
Ga ₂ Te ₃	Cubic	a 5.899	E_{opt} 1.22 (273)
In ₂ Te ₃	Cubic	a 18.486	E_{dir} 1.0 (273)
Sb ₂ Te ₃	Rhombohedral	a 4.25, c 30.35	E_{opt} 0.21 (273)
Bi ₂ Te ₃	Rhombohedral	a 4.384, c 30.487	E_{ind} 0.13 (293)

^a HgTe is a semimetal; the bands overlap.

applications of metal tellurides, the requirements for SSPs and the variety of tellurium-centred ligands that have been used in SSPs. In the second part, the methods used for the generation and characterization of thin films and nanomaterials of metal tellurides will be described, using metal complexes of the recently-developed imino-bis(diisopropylphosphine telluride) ligand as examples.

2 Metal tellurides

Mainly on economic and practical grounds, thin film semiconductors are more extensively employed for practical applications than bulk single crystal materials. The principal II–VI materials have structures closely related to that of ZnS (cubic or hexagonal). These materials have a wide range of band gaps and the direct-transition nature of the materials makes them suitable for use in optical and optoelectronic devices. For example, cadmium telluride (CdTe) possesses a band gap of 1.5 eV and has a range of applications including as

photovoltaic materials, and in gamma-ray detection or X-ray imaging. The exceptional properties of CdTe, such as a high absorption coefficient and a high energy radiation resistance, make it an excellent candidate for solar cells.

Several structural types are found for III–VI compounds, including a defect wurzite structure for Ga₂E₃ (E = S, Se, Te), a defect spinel for In₂E₃ and layered structures for compounds of stoichiometry ME. These sesquichalcogenides are direct band gap semiconductors. Consequently, III–VI materials are potential alternatives to II–VI materials in optoelectronic and photovoltaic devices, but they also have a potential application as passivating layers for III–V devices.³ However, their polytypism and the variety of stoichiometries accessible present more severe problems than those encountered in II–VI materials. The majority of III–VI materials are mid to wide band gap semiconductors, with a direct electronic transition to the conduction band (see Table 1). For example, indium sesquitelluride (In₂Te₃) has been investigated for potential applications in thermoelectric power generators, gas



Mohammad Afzaal

Mohammad Afzaal graduated from Aston University, Birmingham in 2000 and moved to University of Manchester to carry out his PhD with Professor Paul O'Brien, studying growth of semiconductor thin films using single-source precursors. After completing his PhD in 2003, he remained with Professor Paul O'Brien and took his current post-doctoral position, studying nanoparticles and thin film deposition.

Paul O'Brien has been since 1999 Professor of Inorganic Materials Chemistry in the School of Chemistry and the School of Materials at University of Manchester and is at present Head of the School of Chemistry. He was Research Dean in the Faculty of Science and Engineering at University of Manchester from 2001–2003. In 2002, he founded Nanoco Ltd to commercialize quantum dot synthesis. He graduated from Liverpool University in 1975, obtained his PhD from the University of Wales, Cardiff in 1978 and was immediately appointed as a lecturer at Chelsea College of Science and



Paul O'Brien

Technology, University of London. During re-structuring of the University, he moved to Queen Mary and Westfield College in 1984 and was promoted to a chair in 1994. In 1995, he moved to Imperial College of Science, Technology and Medicine as a Professor of Inorganic Chemistry and subsequently as Sumitomo/STS Professor of Materials Chemistry (1997–2003). He was Regents appointed Visiting Professor at Georgia Institute of Technology (1996–1999). He is a Fellow of the Institute of Materials, Minerals and Mining (FIMMM), a Chartered Engineer (C. Eng), corresponding Fellow of the World Innovation Foundation (FWIF). In 2001, he received the Potts Medal (distinguished alumnus award University of Liverpool) and in 2005 he gave the A.G. Evans Memorial Medal lecture at Cardiff University. In 2006, he was awarded the first honorary DSc degree from the University of Zululand, South Africa and in 2007 is the Kroll Medal and Prize Winner for the IOMMM.

sensors, strain gauges and switching memory elements. In_2Te_3 is a layered semiconducting compound which exhibits two crystalline phases. The high temperature phase (above 523 K) is disordered $\beta\text{-In}_2\text{Te}_3$, which has a defect zinc blende structure with a lattice parameter of 0.616 nm, whereas the low temperature $\alpha\text{-In}_2\text{Te}_3$ phase has a defect anti-fluorite structure with a lattice parameter of 1.854 nm.⁴ These two phases are characterized by one-third or two-thirds of the sites of the indium sub-lattice being vacant, respectively.

The V–VI materials E_2Te_3 (E = Sb, Bi) and their alloys are well known for their low-temperature thermoelectric properties and are employed in conventional thermoelectric generators and coolers.⁵ Thermoelectricity is a phenomenon which results from the direct conversion of heat into electricity (Seebeck effect) and *vice versa* (Peltier effect). The performance of thermoelectric materials and devices is quantified by the dimensionless figure of merit parameter (ZT):

$$ZT = \alpha^2/\rho\lambda$$

Where α is the Seebeck coefficient, ρ the electrical resistivity and λ the thermal conductivity.⁶ Good thermoelectric properties are achieved for a high ZT value, which is associated with a high α -value and low ρ - and λ -values. Both Sb_2Te_3 and Bi_2Te_3 are narrow band gap semiconductors, which have rhombohedral structures with a space group of $R\bar{3}m$ (Fig. 1a). By transformation of axes, the unit cell can also be described as hexagonal with three asymmetric units (Fig. 1b).

The electrical and optical properties of semiconductor layers are critically dependent on the nature and purity of the precursor. It has been possible to use the correlation between precursor purity and layer properties to develop and, most importantly, monitor efficient purification routes to ultra-high purity compounds. The nature of the precursor and its decomposition characteristics heavily influence the incorporation of intrinsic impurities (*e.g.* carbon, phosphorus) into the layer, whilst extrinsic impurities (*e.g.* trace metal, solvent) can vary, depending on the synthesis and purification routes

employed. Carbon incorporation is, therefore, strongly dependent on the molecular structure of the precursor. The presence of volatile trace metal impurities in the precursors leads to the incorporation of shallow, ionized impurities in the semiconductor layer. These impurities have energies which place them in the band gap of the II–VI or III–VI layer, and thus seriously degrade the semiconductor properties by lowering the electron mobility.

3 Requirements for single-source precursors

Single-source precursors often have numerous advantages over conventional precursors, including: air and moisture stability, ease of handling, comparatively low toxicity and often lower growth temperatures. The presence of only one precursor molecule in the supply stream reduces the likelihood and extent of pre-reaction and the associated contamination of deposited film, and permits intrinsic control of film stoichiometry. Ligand design allows a degree of control over both the type and the level of impurities incorporated into the films such as carbon from an alkyl group. Furthermore, in some precursors, such as molecular cluster compounds, the phase of the deposited material can be controlled by the core structure of the precursor molecule. Despite the numerous potential advantages of SSPs, these compounds are not without drawbacks. The high molecular weights tend to lead to lower volatility which can be problematic in conventional atmospheric pressure CVD. This problem is exacerbated in systems requiring two or more metals, since the presence of additional metal would increase the molecular weight. However, it can be overcome by using a low-pressure environment, or by employing a solution of the precursor as in aerosol-assisted chemical vapour deposition (AACVD) (see Section 6) or liquid injection CVD. A further problem associated with SSPs is the difficulty in depositing materials with defined non-integral stoichiometries or when dopants are required.

4 Tellurium-centred ligands

A significant challenge in the design and synthesis of suitable SSPs for metal tellurides is the fact that tellurium analogues of ligands that are often used as sulfur- or selenium-containing precursors are either unknown, *e.g.* ditellurocarbmates $[\text{R}_2\text{NCTe}_2]^-$, or not readily available, *e.g.* tellurocarboxylates $[\text{RC(O)Te}]^-$.² Tellurolates are potentially important precursors for the generation of tellurides.⁸ However, tellurols are generally considered to be undesirable reagents on account of their foul smell, toxicity and thermal instability. Furthermore, metal tellurolates are commonly non-volatile, polymeric compounds. These objections can be overcome, however, by the use of very bulky groups, as in the remarkably stable tellurol $[(\text{Me}_3\text{Si})_3\text{Si}]_2\text{TeH}$ (**1**, mp 128–130 °C) or the sterically hindered benzenetellurols **2a–c** which, unlike PhTeH , can be isolated as colourless low melting solids.⁹

Group 12 metal complexes of **1** and **2a–c** are obtained by treatment of an organometallic reagent, *e.g.* Et_2Zn or a metal amide, *e.g.* $\text{M}[\text{N}(\text{SiMe}_3)_2]_2$ (M = Zn or Cd), with the tellurol.⁹ The gas-phase pyrolysis of such complexes produces crystalline films of the corresponding binary tellurides. For example,

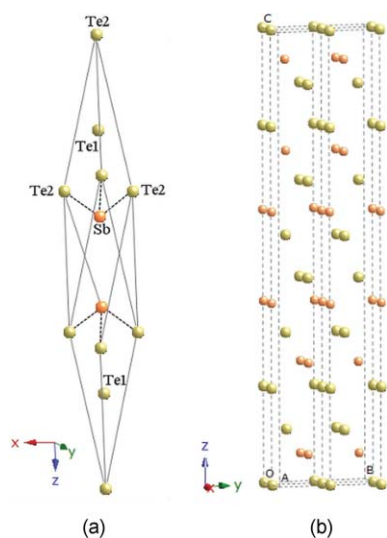
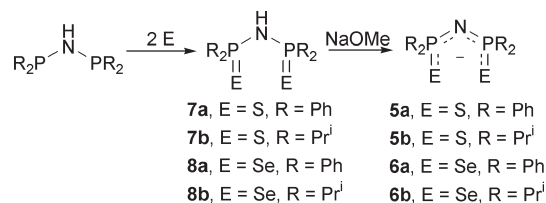
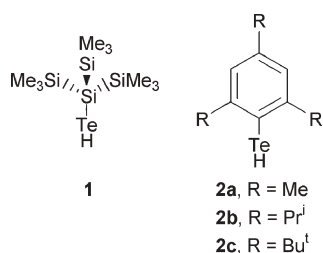


Fig. 1 (a) Rhombohedral unit cell and (b) hexagonal unit cell of Sb_2Te_3 .



Scheme 2

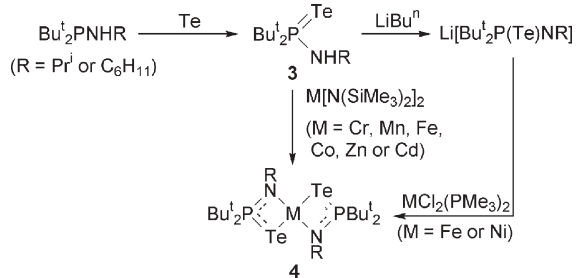
Arnold *et al.* have shown that the group 12 tellurides MTe (M = Zn, Cd, Hg) may be obtained in this manner from $M[\text{Te}\{\text{Si}(\text{SiMe}_3)_3\}]_2$.¹⁰ Similarly, thermolyses of the group 14 complexes $M[\text{Te}\{\text{Si}(\text{SiMe}_3)_3\}]_2$ (M = Sn, Pb) at 250 °C proceed cleanly to give cubic SnTe and PbTe containing small amounts of carbon.¹¹ Another example of the attempted use of telluroate complexes as SSPs for metal tellurides is the production of impure In_2Te_3 by heating the dimer $[(\text{mes})_2\text{In}(\mu\text{-TePh})]_2$ (mes = mesityl) at 600 °C.¹²

Bochmann *et al.* have developed an alternative to the telluroate-based route to metal tellurides that involves the synthesis, and subsequent thermolysis, of chelate complexes of phosphine tellurides of the type $\text{Bu}^t_2\text{P}(\text{Te})\text{NHR}$ (**3**, R = Prⁱ, C₆H₁₁). The general approach is illustrated in Scheme 1. The thermally stable, sublimable complexes **4** (M = Zn, Cd) have been used to grow thin films of group 12 tellurides free from phosphorus contamination.¹³

Compounds containing the metal and tellurium atoms arranged in a ring system are also potential candidates as SSPs. For example, Boudjouk *et al.* have used the six-membered ring $(\text{Bn}_2\text{SnTe})_3$ to generate phase-pure cubic SnTe.¹⁴

5 Imino-bis(diisopropylphosphine chalcogenides)‡

From the foregoing discussion of tellurium-centred ligands, it is evident that there is scope for an alternative ligand system that forms metal complexes which possess the desirable characteristics of potential SSPs and that would also be applicable for the generation of a wide range of metal telluride thin films. In 2002, O'Brien *et al.* showed that the metal complexes of the monoanionic imino-bis(diphenylphosphine chalcogenide) ligands $[\text{N}(\text{PPh}_2\text{E})_2]^-$ (Scheme 2, **5a**, E = S; **6a**, E = Se) are suitable SSPs for the group 12 metal



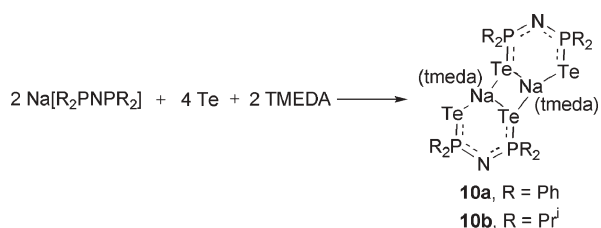
Scheme 1

chalcogenides.¹⁵ Since a wide range of metal complexes of these bidentate inorganic ligands are known and easily prepared,¹⁶ this discovery paved the way for the generation of thin films of a wide variety of metal chalcogenides from homoleptic complexes of **5** and **6** by using AACVD techniques. In CVD applications, complexes of the isopropyl derivatives **5b** and **6b** are preferred in view of their higher volatility compared to that of the phenyl-substituted analogues **5a** and **6a**. Some pertinent examples include selenides of group 13 (Ga and In),¹⁷ group 14 (Pb),¹⁸ and group 15 (Sb and Bi).^{19,20} Heteroleptic organometallic derivatives of the type $\text{RM}[\text{N}(\text{PPr}^i_2\text{E})_2]$ (M = Cd, E = Se, R = Me; M = Hg, E = S, Se; R = Me, Et, 2-thienyl, 2-selenyl, Ph) have also been used to generate CdSe²¹ and HgE (E = S, Se).²² However, the potential generation of toxic Me_2Se is an undesirable feature of these SSPs. In an interesting adaptation of this approach, thin films of I/III/VI semiconductors, *e.g.* CuInSe_2 ,²³ have been deposited by thermolytic decomposition of $\text{Cu}[\text{N}(\text{PPr}^i_2\text{Se})_2]$ in the presence of the indium precursor $\text{In}[\text{N}(\text{PPr}^i_2\text{Se})_2]_2\text{Cl}$. These ternary materials are of considerable interest in photovoltaic applications.

The diseleno PNP ligands **8a** and **8b** are prepared using methodology developed by Woollins *et al.* (see Scheme 2).²⁴ These neutral ligands are readily deprotonated to the monoanions **6a** and **6b** by treatment with bases such as sodium methoxide.²³ Subsequent metathetical reactions of **6a** or **6b** with metal halides produce homoleptic complexes in good yields.¹⁶

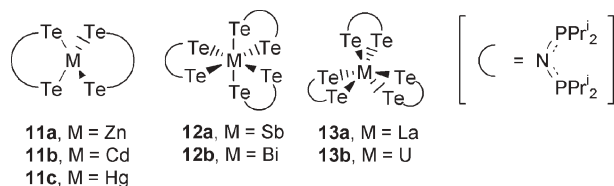
Ditelluro analogues of the neutral ligands **7** and **8** are not available by the route shown in Scheme 2. The oxidation of the phosphorus(III) systems $\text{R}_2\text{PN}(\text{H})\text{PR}_2$ does not occur to a significant extent in the case of R = Ph, even in boiling toluene.²⁵ The isopropyl derivative $\text{Pr}^i_2\text{PN}(\text{H})\text{PPr}^i_2$ is oxidized by tellurium at room temperature to the monotelluride, which is isolated in 81% yield as the P–H tautomer $\text{Pr}^i_2\text{P}(\text{H})\text{NPPr}^i_2\text{Te}$ (**9**).²⁶ However, further oxidation of **9** with tellurium is not possible. In 2002, Chivers *et al.* developed an alternative strategy for the synthesis of the desired ditelluro PNP ligand that involves metallation of the phosphorus(III) reagents $\text{R}_2\text{PN}(\text{H})\text{PR}_2$ with sodium hydride *prior to reaction with elemental tellurium*. The installation of a formal negative charge renders the phosphorus(III) centres more nucleophilic towards tellurium. As depicted in Scheme 3, this methodology facilitated the synthesis of the ditelluro PNP ligand as the sodium salt (**10a**, R = Ph), which forms a centrosymmetric dimer in the solid state.²⁶ This new synthetic protocol was later shown to be applicable to the sodium salt of the isopropyl-substituted ligand **10b**, which is of more interest in SSP work (*vide supra*).²⁷

‡ For simplicity, imino-bis(dialkylphosphine chalcogenides) will be referred to as dichalcogeno PNP ligands in the text of this article.



Scheme 3

The availability of the ditelluro PNP ligand as the sodium salt **10b** has paved the way for the preparation of a wide variety of homoleptic metal complexes for investigations of their suitability as SSPs to metal tellurides. For example, the Zn, Cd and Hg complexes (**11a–c**) with distorted tetrahedral structures are obtained in good yields from metathetical reactions of **10b** with metal dihalides.²⁷ The antimony and bismuth complexes (**12a** and **12b**) have been prepared in a similar manner and shown to have distorted octahedral structures. The generality of this approach is further illustrated by the report of Gaunt *et al.* of the synthesis of lanthanum(III) and uranium(III) complexes (**13a** and **13b**) from the reactions of **10b** and the appropriate metal triiodides.²⁸ The complexes **13a** and **13b** exhibit distorted trigonal prismatic structures. The uranium complex **13b** is the first example of a molecular compound containing an actinide–tellurium bond.



Although homoleptic complexes of the coinage metals may be obtained by metathetical reactions, the strong reducing power of the ditelluro PNP ligand is readily evident in the formation of a gold mirror upon reaction of **10b** with AuCl.²⁹ In the presence of triphenylphosphine, however, the monomeric gold complex **14** is stabilized and can be isolated in good yields. Metathesis of **10b** with CuCl produces the trimeric copper complex **15** whose structure differs significantly from that of the corresponding selenium complex **16**.²³ All three ligands in **16** are coordinated to the copper centre *via* one two-coordinate and one three-coordinate chalcogen donor to give a symmetrical Cu₃Se₃ ring. By contrast, only two of the ligands adopt this mode of coordination in **15**; the third acts as a bridging ligand with two three-coordinate tellurium sites leading to close contacts for two of the Cu–Cu interactions.²⁹

Metathesis of **10b** with AgI also proceeds in a straightforward manner to give the homoleptic complex **17**,²⁹ which

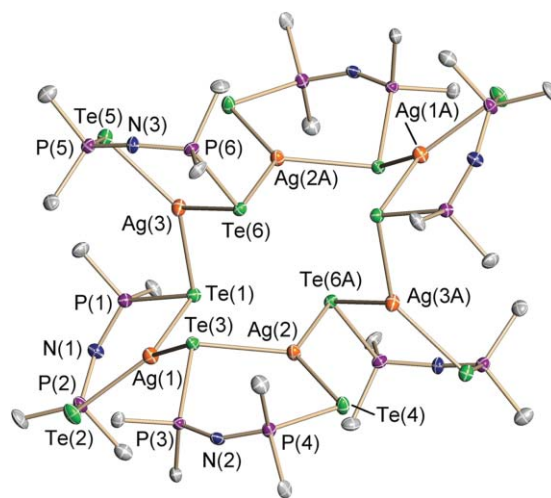
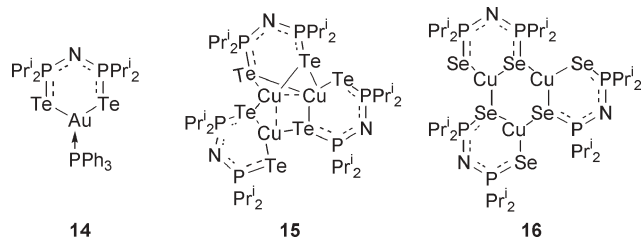
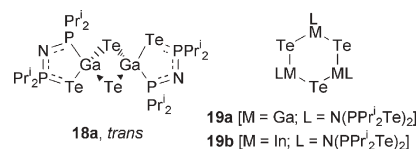


Fig. 2 Molecular structure of $\{\text{Ag}[\text{N}(\text{Pr}^i_2\text{P}\text{Te}_2)]_6$ (**17**) (ref. 29—Reproduced by permission of The Royal Society of Chemistry).

exhibits an unprecedented twelve-membered ring structure (Fig. 2); the corresponding selenium complex is trimeric.²³

In contrast to the formation of homoleptic complexes in metathetical reactions of **10b** with group 11, 12 or 15 halides and with lanthanum or uranium triiodides, the reaction of **10b** with group 13 trihalides resulted in novel tellurium-transfer reactions. Thus treatment of **10b** with gallium trichloride in a 1 : 1 molar ratio produced complex **18** containing a central Ga₂Te₂ ring and the monotelluride ligand $[\text{Pr}^i_2\text{PNPPPr}^i_2\text{Te}]^-$, which is P,Te-chelated to the gallium centres.³⁰ Although this complex is isolated as the *trans*-isomer **18a**, ³¹P NMR data indicate that the *cis*-isomer **18b** is also present in solution.³⁰ The reaction of indium trichloride with **10b** provides another example of tellurium transfer. In this case, however, the isolated product **19b** consists of a central six-membered In₃Te₃ ring stabilized by chelation of a ditelluro PNP ligand to each indium centre.³⁰



Since some of the N(PPRⁱ₂Te)₂ ligands serve as a sacrificial source of telluride in the formation of the In₃Te₃ ring, complex **19b** is obtained in low yield. In view of the potential interest in this metallacycle as a SSP for indium telluride, Chivers and Copsey developed an alternative synthesis that involves the reaction of **10b** with indium(I) chloride in the presence of elemental tellurium.³⁰ This *in situ* self-assembly produces **19b** in 75% yield. A similar method can be used for the synthesis of the analogous Ga₃Te₃ ring system **19a** by using “GaI” rather than InCl.³⁰

6 CVD techniques

The deposition of semiconducting thin films can be performed on various substrates by using numerous techniques, mainly belonging to two families: (a) physical vapour deposition

(PVD) and (b) chemical vapour deposition (CVD). Most metallisation for microelectronics today is performed by PVD, which includes evaporation and sputtering. In both methods, the formation of a layer on a substrate involves three steps: (1) conversion of a condensed-phase material (often a solid) into the gaseous or vapour phase, (2) transportation of the gaseous phase from the source to the substrate surface, followed by (3) nucleation and growth of a new layer.

Chemical vapour deposition (CVD) is a generic name for a range of processes used for the deposition of thin solid films, in which a volatile molecular species is transported into the reactor that contains substrates where the molecular species adsorbs and reacts to deposit a film of a particular material.^{31,32} Features common to all CVD reactors include: source evaporators with an associated gas-handling system to control input gases and gas-phase precursor concentration, a reactor cell with a heated susceptor, and an exhaust system to remove waste products (which may include a vacuum pump for low-pressure operations). The basic physicochemical processes which underline a CVD process in general are shown schematically in Fig. 3 and can be summarized as follows:

- Mass transport of reagents in the bulk gas flow region to the deposition zone.
- Gas-phase reaction in the boundary layer which produces film precursors and by-products.
- Mass transport of film precursors through the boundary layer to the growth surface.
- Adsorption of film precursors on the substrate or growing film surface.
- Surface diffusion of the precursors to growth sites.
- Surface chemical reactions leading to film deposition and to by-products, which subsequently desorb.
- Mass transport of by-products into the bulk gas flow region and out of the reactor.

The mechanisms of the deposition process are of crucial importance in determining the quality of the layers grown and whether or not growth is optimal. The surface chemistry of these systems is under intense study and is beyond the scope of this review.

The major differences between the various CVD techniques are related to the initiation of mass transport. In conventional CVD, volatile precursors are delivered from bubblers or gases from cylinders often at low pressure (LP) in the reactor for

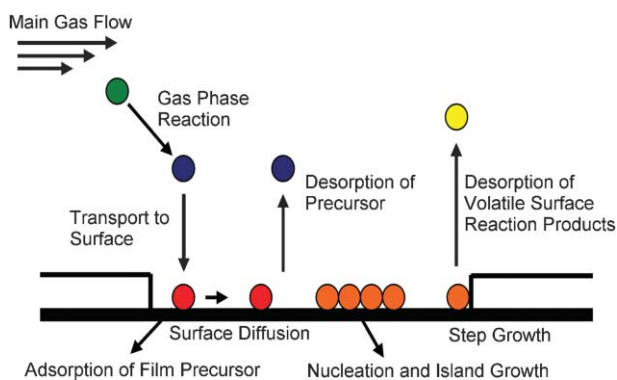


Fig. 3 Transport and reaction processes in CVD.³

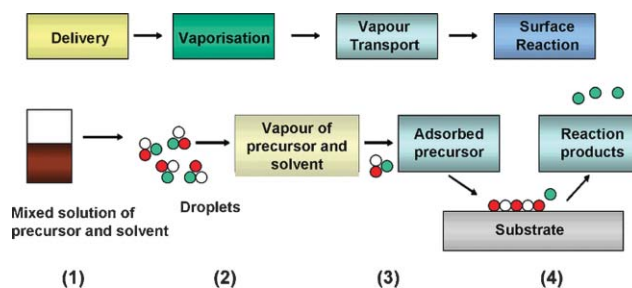


Fig. 4 Schematic representation of the AACVD process.

safety reasons. Additionally, kinetic steps are often aided under LPCVD conditions.³³ When solid precursors are used, good mass transport rates rely, in the large part, on the precursor having a suitable vapour pressure. The problem of unfavourable precursor sublimation characteristics can be circumvented by using a method such as aerosol-assisted CVD (AACVD). The four-stage AACVD process is illustrated in Fig. 4. The precursors are dissolved in an organic solvent (1) and are converted into droplets by a piezoelectric modulator (2). The aerosol of precursor and solvent is then transported by a carrier gas into a hot zone where it evaporates. The vapour of the precursors is then transported to the substrate where it adsorbs and reacts to form a film and by-products (3) and (4).

In general, aerosol delivery systems are suitable when the precursor has low volatility, or if it is thermally unstable and would decompose if heated for prolonged times, to elevate the vapour pressure. It is also a useful technique for multi-component systems since the relative transport rates of the precursors depend solely on their concentrations in the precursor solution. In contrast, LPCVD and/or conventional CVD rely on the delivery of the precursor at its equilibrium vapour pressure at the source temperature.

7 Materials characterization techniques

The physical properties of a solid material are determined by its extended crystallographic structure and microstructure, as well as the presence of defects and/or impurities or dopants. The proper characterization of a solid is therefore of critical importance if it is to realize applications in electronic devices, for which reproducible properties are vital. Materials characterization involves the identification of the elements present, their crystallographic arrangement and the microstructure of the material. A solid is often an aggregate of random or oriented crystal grains (crystallites), which are often between 10^{-8} and 10^{-6} m in diameter.

7.1 Powder X-ray diffraction

Powder X-ray diffraction (PXRD) is often used to identify the phase of a material and the unit cell parameters; it can also provide information on the presence of structural imperfections and/or strains. In powders, the crystalline domains are arranged to be randomly oriented to record the 2-dimensional PXRD pattern which shows concentric rings of diffraction peaks (called Debye rings) with radii corresponding to the d -spacings of (hkl) planes in the crystal lattice.³⁴ The phase of the thin film sample can be derived from analyzing the

position, intensity and indexing of the diffracted peaks. There are several considerations in using PXRD to characterize thin film samples. Reflectional methods are generally used for the measurements as the substrates are generally too thick for transmission. High angular resolution is often required because the peaks from semiconductor materials can be sharp due to very low defect densities in the material. Consequently, multiple bounce crystal monochromators are often used to provide a highly collimated X-ray beam for the measurements.³⁴ For most applications, the amount of information that can be extracted depends on the nature of the sample microstructure (crystallinity, structural imperfections, crystal grain size, texture), the complexity of the crystal structure (number of atoms in the asymmetric unit, unit cell volume) and the quality of the experimental data (instrument performance, counting statistics).

7.2 Scanning electron microscopy

The scanning electron microscope (SEM, sometimes called 'secondary electron microscope') provides information relating to topographical features, morphology, crystal structure, crystal orientation and compositional differences. It uses electrons for imaging, much as a light microscope uses visible light. This gives rise to two of the major benefits of the SEM: range of magnification and depth-of-field in the image. Depth-of-field is the property of SEM images where surfaces at different distances from the lens appear in focus, giving 3-dimensional information.³⁵ The SEM has more than 300 times the depth-of-field of the light microscope. Another important advantage of the SEM over the optical microscope is its high resolution. Resolution of 1 nm is achievable from a SEM with a field emission gun (FEG). In SEM, an incident electron beam is raster-scanned across the surface of the sample. Electrons of varying energies are emitted from the sample, including high energy back-scattered electrons and Auger electrons (arising from ionisation of the sample surface), but normally secondary electrons (those arising from inelastic collisions with surface atoms) are recorded by a detector and used to generate the SEM image. Imaging is typically obtained using secondary electrons for the best resolution of fine surface topographical features. For secondary electron imaging, thin films must be electrically conductive. Nonconductive thin film materials can be evaporatively coated with carbon or gold to obtain conductivity without affecting the observed surface morphology.

7.3 Energy dispersive X-ray microanalysis

Besides the imaging of surfaces, the scanning electron microscope offers the possibility to determine the elemental composition of the sample quantitatively with the help of an additional detector for energy dispersive X-ray microanalysis (EDAX) attached to the SEM. In addition to low energy secondary electrons and back-scattered electrons, X-rays are also generated when materials are irradiated with an electron beam.³⁵ The high energy incident electrons excite core-level electrons in surface atoms to higher energy shells. When the excited electrons relax back to the lower energy shells, they emit electromagnetic radiation in the form of X-rays. The

wavelengths, and hence energies, of the X-rays are characteristic of the electron shell energies, and the spectrum can be used to distinguish different elements. It is possible to measure the relative amount of each element present from the spectrum, and the X-ray spectrum produced in tandem with the SEM can therefore be used to determine the elemental composition of materials.

7.4 Transmission electron microscopy

A transmission electron microscope (TEM) operates on the same basic principles as a light microscope. It is based on the fact that the incident electron beam is of sufficient energy to propagate through the specimen (<100 nm thick). A series of electromagnetic lenses then magnifies the transmitted electron signal. Diffracted electrons are observed using a detector beneath the specimen and take the form of a selected area electron diffraction (SAED) pattern. This information can be used to determine the atomic structure of the material in the sample. Transmitted electrons can also form images from small regions of the sample that contain contrast, due to several scattering mechanisms associated with interactions between electrons and the atomic constituents of the sample.³⁶ Analysis of the transmitted electron images yields information about the microstructure, *e.g.* the grain size, and crystallographic structure of a sample at an atomic level. Due to its high resolution, TEM is an invaluable tool to study nanoscale properties of crystalline materials such as semiconductors and metals.

8 Metal complexes of imino-bis(diisopropylphosphine telluride) as sources for metal tellurides

In this final section, the use of metal complexes of imino-bis(diisopropylphosphine telluride) as single-source precursors to thin films of metal tellurides will be illustrated using several recent examples. The first involves the generation of CdTe, a low band gap semiconductor (*ca.* 1.5 eV) that is of interest for use in photovoltaic devices. The AACVD of Cd[N(PPrⁱ₂Te)₂]₂ (**11b**) on glass substrates produces CdTe films whose composition is temperature-dependent.³⁷ At lower temperatures, a mixture of cubic CdTe and hexagonal Te is obtained, whereas in the temperature range 425–475 °C pure CdTe films are produced (Fig. 5). The morphology of these films is not dependent on growth temperature. At all temperatures, the orientation of CdTe was along the [111] direction. By contrast, the AACVD of Hg[N(PPrⁱ₂Te)₂]₂ (**11c**) under similar conditions produces hexagonal tellurium. This observation has been tentatively explained as resulting from the reductive elimination of the ligand from the metal centre, with consequent formation of the ditelluride dimer (TePPrⁱ₂NPPrⁱ₂Te)₂ and elemental Hg. Under the experimental conditions, the dimeric species decomposes to give the observed elemental Te.

The second example is the synthesis of Sb₂Te₃ nanoplates. Antimony telluride, Sb₂Te₃, and its bismuth analogue are layered semiconductors with narrow band gaps that are widely used in thermoelectric generators and refrigerators. The application of the AACVD technique to the homoleptic

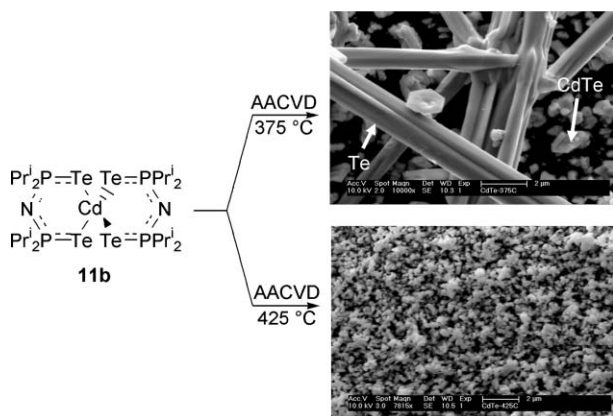


Fig. 5 AACVD of **11b** (ref. 37—Reproduced by permission of the Royal Society of Chemistry).

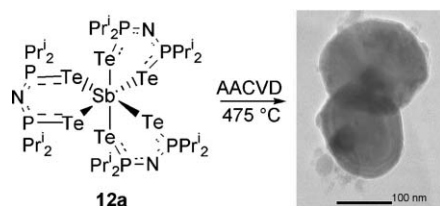


Fig. 6 AACVD of **12a** (Reprinted with permission from ref. 38. Copyright (2006) American Chemical Society).

antimony(III) complex $\text{Sb}[\text{N}(\text{PPr}_2^i\text{Te})_2]_3$ (**12a**) in the temperature range 375–475 °C produces hexagonal-shaped nanoplates of pure rhombohedral Sb_2Te_3 (Fig. 6).³⁸ Surface analysis of these films by FEG-SEM showed that the growth temperature does not effect the morphologies of the deposited film. The purity of the Sb_2Te_3 thin films produced in this manner may be contrasted with the recent report by Wang *et al.*³⁹ of the solvothermal synthesis of Sb_2Te_3 that is contaminated with elemental tellurium.

Thin films of III–VI materials such as In_2Te_3 (band gap 1.0 eV) are potential alternatives to II–VI semiconductors for applications in optoelectronic and photovoltaic devices. The AACVD of complex **19b** in the temperature range 375–475 °C on glass and Si (100) substrates gave black, uniform films of cubic In_2Te_3 (Fig. 7).⁴⁰ SEM showed that the morphology of the films does not vary significantly with an increase in deposition temperature, but the grain size increases. This was the first report of pure cubic In_2Te_3 films generated from a molecular precursor. Although the indium complex **19b** gave

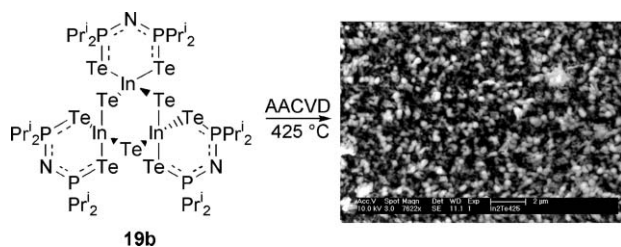
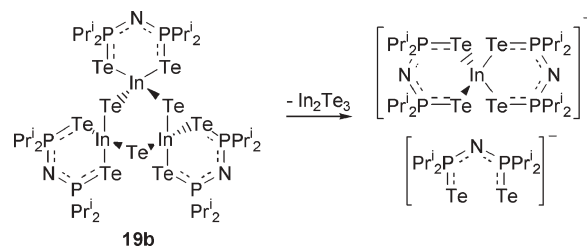


Fig. 7 AACVD of **19b** (ref. 40—Reproduced by permission of the Royal Society of Chemistry).



Scheme 4

In_2Te_3 exclusively, the analogous gallium complex **19a** produces a mixture of Ga_2Te_3 and hexagonal tellurium.

Some insight into the fragmentation process that generates In_2Te_3 was provided by the electrospray mass spectrum (ESMS) of **19b** in dilute THF solutions.⁴⁰ The molecular ion was not observed, but a band of peaks with isotopic patterns appropriate for the homoleptic indium cation $\{\text{In}[\text{N}(\text{PPr}_2^i\text{Te})_2]_2\}^+$ together with a fragment anion corresponding to the ligand $[\text{N}(\text{PPr}_2^i\text{Te})_2]$, which is detected as the diprotonated species in the ESMS, dominated the spectrum. On this basis, it was inferred that the deposition of In_2Te_3 occurs directly from the central In_3Te_3 ring of **19b** as depicted in Scheme 4.

Copper and silver tellurides are promising materials for solar cells, photodetectors, thermoelectronic or magnetic devices. Group 11 complexes such as $\{\text{Cu}[\text{N}(\text{PPr}_2^i\text{Te})_2]\}_3$ (**15**) and $\{\text{Ag}[\text{N}(\text{PPr}_2^i\text{Te})_2]\}_6$ (**17**) are well-suited for AACVD experiments because of their high molecular masses.²⁹ The films deposited from the copper precursor **15** at 300–500 °C were non-adherent to the substrates and comprised of a mixture of CuTe , Te and P . The morphologies of the films consisted of CuTe sheets along with Te rods. The AACVD of the hexameric silver complex **17** resulted in the formation of both Ag_7Te_4 and Te at 300–500 °C on glass (Fig. 8). At the lowest growth temperature (300 °C), the formation of micron-sized tellurium tubes along with truncated hexagonal plates and spheres of Ag_7Te_4 was observed. At 350–500 °C, spherical particles were produced and energy dispersive X-ray analysis (EDAX) indicated silver-deficient and tellurium-rich films along with traces of phosphorus. The presence of phosphorus indicates incomplete decomposition of compound **17** in this temperature regime. At 500 °C, EDAX analysis revealed high tellurium content within the films with no phosphorus contamination. In all cases, tellurium-rich films are a consequence of the formation of a mixture of both Te and Ag_7Te_4 as elaborated by PXRD. The possible evaporation of silver from the surface of films may account for the silver-deficient films. At the highest deposition temperature, the

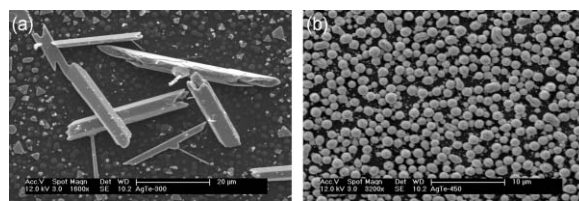


Fig. 8 SEM images of (a) a mixture of Ag_7Te_4 and Te tubes at 300 °C and (b) Ag_7Te_4 at 450 °C (ref. 29—Reproduced by permission of The Royal Society of Chemistry).

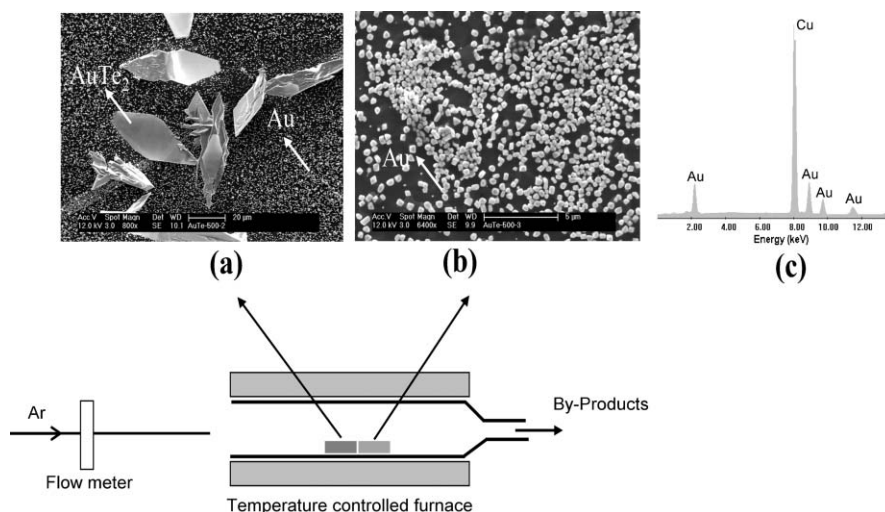


Fig. 9 Deposition of (a) mixture of AuTe₂ and Au, and (b) Au films. (c) EDAX pattern of Au films at 500 °C.

absence of phosphorus contamination in the films is possibly due to the rupture of Te–P bonds.

Attempts were made to deposit gold telluride thin films from the monomeric gold complex Au(PPh₃)[N(PPrⁱ₂Te)₂] (**14**) on glass at 300–500 °C.²⁹ At 300 °C, only monoclinic AuTe₂ films were deposited, whereas at a higher temperature (350 °C) a mixture of monoclinic AuTe₂ and cubic Au films was formed. With a further increase in growth temperature to 400–500 °C, two types of deposits were observed: a mixture of monoclinic AuTe₂ and an Au film closest to the precursor inlet (the cooler part of the reactor, Fig. 9a) and only a cubic Au film further away from the precursor inlet (Fig. 9b). The EDAX pattern of the Au film is shown in Fig. 9c; the Cu signal is due to the copper grid used in TEM studies. At deposition temperatures >350 °C, the formation of individual gold particles along with AuTe₂ is due to the depletion of tellurium under CVD conditions. Gold has a high affinity for tellurium because of its soft character, resulting in the formation of AuTe₂ followed by Au particles.

SEM studies showed that the films grown at 300–350 °C consist of granules with a broad distribution of sizes and morphologies. At 400–500 °C, the films are comprised of micrometer-sized parallelepiped AuTe₂ along with anisotropic gold microstructures. The gold films are composed of well-defined faceted crystals including triangular, cubic and polyhedral particles. Some gold particles seem to be agglomerates of two, three, or more smaller particles (Fig. 10a). The corresponding selected area electron diffraction (SAED) pattern generated from particles confirms their single crystallinity (Fig. 10b). The UV-visible absorption spectra of the gold films formed at 400–500 °C showed a broad absorption band at 554 nm, indicating high polydispersity, both in size and shape.

9 Conclusions and prospects

This *tutorial review* has given the reader an introduction to the preparation of metal telluride thin films through the use of SSPs. These materials can be used in electronic devices such as solar cells and infrared detectors. Several research groups have

successfully used tellurium-based ligands in combination with various main group metals in molecular precursors to thin films and nanoparticles of these materials. The review has focused on metal complexes of the recently developed iminobis(diisopropylphosphine telluride) ligand which, in the case of homoleptic compounds, are easily prepared by metathesis reactions with metal halides. These crystalline precursors have been used in AACVD experiments to generate pure thin films of CdTe, Sb₂Te₃, and In₂Te₃. By contrast, group 11 complexes of this ligand yield thin films of coinage metal tellurides that are often contaminated with tellurium or phosphorus.

The synthesis of thin films by CVD processes can be facilitated by volatilisation techniques such as LPCVD and AACVD, and these modifications are useful when the precursors have low volatility and/or thermal instability. The characterization of solid-state materials is performed using techniques such as PXRD, SEM and TEM. We hope to have given the reader an appreciation for the most important tools available for the qualitative and quantitative analysis of the surface or bulk phase of a solid.

The outlook for the SSP approach in terms of commercialisation remains to be seen. However, research is underway to develop next-generation precursors to overcome problems such as the non-ideal stoichiometry of metal and chalcogen atoms in the precursor molecule which may cause intrinsic

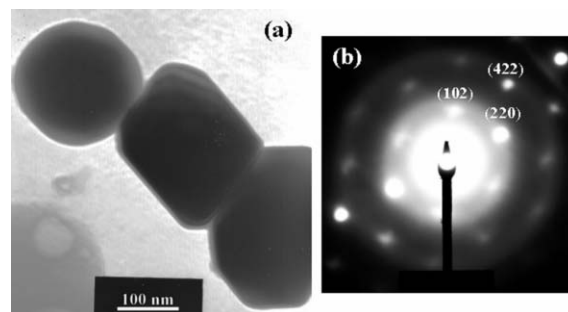


Fig. 10 (a) TEM image of Au particles and (b) corresponding SAED pattern.

impurities (such as elemental Te) in the generated materials. The recent increased interest in main group tellurides make it likely that the future will see the development of improved SSPs to these important materials.

Acknowledgements

Financial support from NSERC (Canada) (TC and JSR), Alberta Ingenuity and the Izaak Walton Killam Memorial Foundation (JSR) and EPSRC (UK) (POB and MA) is gratefully acknowledged. MA and POB would also like to thank Dr Christopher Muryn for helpful discussions concerning crystallography.

References

- 1 M. Afzaal and P. O'Brien, *J. Mater. Chem.*, 2006, **16**, 1597.
- 2 A. N. Gleizes, *Chem. Vap. Deposition*, 2000, **6**, 155.
- 3 A. C. Jones and P. O'Brien, *CVD of Compound Semiconductors: Precursor Synthesis, Development and Applications*, VCH, Weinheim, 1997, ISBN: 3-527-29294-1.
- 4 K. Dovletov, F. Ragimov, S. Nuryev and N. K. Samakhotina, *Soviet Phys.-Semicond.*, 1982, **19**, 770.
- 5 R. Venkatasubramanian, E. Siivola, T. Colpitts and B. O'Quinn, *Nature*, 2001, **413**, 597.
- 6 D. D. Frari, S. Diliberto, N. Stein, C. Boulanger and J.-M. Lecuire, *Thin Solid Films*, 2005, **483**, 44.
- 7 O. Madelung, *Semiconductors – Basic Data*, Springer, Berlin, 2nd edn, 1996, pp. 180–186 and 190–192, ISBN: 3-540-60883-4.
- 8 H. B. Singh and N. Sudha, *Polyhedron*, 1996, **15**, 745.
- 9 T. Chivers, *J. Chem. Soc., Dalton Trans.*, 1996, 1185.
- 10 J. Arnold, J. M. Walker, K. M. Yu, P. J. Bonaria, A. L. Seligson and E. D. Bourret, *J. Cryst. Growth*, 1992, **124**, 647.
- 11 A. L. Seligson and J. Arnold, *J. Am. Chem. Soc.*, 1993, **115**, 8214.
- 12 H. Rahbarnoohi, R. Kumar, M. J. Heeg and J. P. Oliver, *Organometallics*, 1995, **14**, 502.
- 13 G. C. Bwembya, X. Song and M. Bochmann, *Chem. Vap. Deposition*, 1995, **1**, 78.
- 14 P. Boudjouk, M. P. Remington, Jr., D. G. Grier, W. Triebold and B. R. Jarabek, *Organometallics*, 1999, **18**, 4534.
- 15 M. Afzaal, S. M. Aucott, D. Crouch, P. O'Brien, J. D. Woollins and J.-H. Park, *Chem. Vap. Deposition*, 2002, **8**, 187.
- 16 C. Silvestru and J. E. Drake, *Coord. Chem. Rev.*, 2001, **223**, 117.
- 17 J.-H. Park, M. Afzaal, M. Helliwell, M. A. Malik, P. O'Brien and J. Raftery, *Chem. Mater.*, 2003, **15**, 4205.
- 18 M. Afzaal, K. Ellwood, N. L. Pickett, P. O'Brien, J. Raftery and J. Waters, *J. Mater. Chem.*, 2004, **14**, 1310.
- 19 J. Waters, D. Crouch, J. Raftery and P. O'Brien, *Chem. Mater.*, 2004, **16**, 3289.
- 20 D. J. Crouch, M. Helliwell, P. O'Brien, J.-H. Park, J. Waters and D. J. Williams, *Dalton Trans.*, 2003, 1500.
- 21 M. Afzaal, D. Crouch, M. A. Malik, M. Mottevali, P. O'Brien and J.-H. Park, *J. Mater. Chem.*, 2003, **13**, 639.
- 22 D. J. Crouch, P. M. Hatton, M. Helliwell, P. O'Brien and J. Raftery, *Dalton Trans.*, 2003, 2761.
- 23 M. Afzaal, D. J. Crouch, P. O'Brien, J. Raftery, P. J. Skabara, A. J. P. White and D. J. Williams, *J. Mater. Chem.*, 2004, **14**, 233.
- 24 D. Cupertino, D. J. Birdsall, A. M. Z. Slawin and J. D. Woollins, *Inorg. Chim. Acta*, 1999, **290**, 1.
- 25 G. G. Briand, T. Chivers and M. Parvez, *Angew. Chem., Int. Ed.*, 2002, **41**, 3468.
- 26 T. Chivers, D. J. Eisler, J. S. Ritch and H. M. Tuononen, *Angew. Chem., Int. Ed.*, 2005, **44**, 4953.
- 27 T. Chivers, D. J. Eisler and J. S. Ritch, *Dalton Trans.*, 2005, 2675.
- 28 A. J. Gaunt, B. L. Scott and M. P. Neu, *Angew. Chem., Int. Ed.*, 2006, **45**, 1638.
- 29 M. C. Copesey, A. Panneerselvam, M. Afzaal, T. Chivers and P. O'Brien, *Dalton Trans.*, 2007, 1528.
- 30 M. C. Copesey and T. Chivers, *Chem. Commun.*, 2005, 4938.
- 31 L. V. Interrante and M. J. Hampden-Smith, *Chemistry of Advanced Materials, An Overview*, Wiley-VCH, New York, 1998, p. 176.
- 32 For a recent review of the formation of metal oxide and metal nitride thin films by CVD, see: L. McElwee-White, *Dalton Trans.*, 2006, 5327.
- 33 M. Lazell, P. O'Brien, D. J. Otway and J.-H. Park, *J. Chem. Soc., Dalton Trans.*, 2000, 4479.
- 34 P. W. Atkins, *Physical Chemistry*, Oxford University Press, New York, 6th edn, 1998, pp. 625–627.
- 35 J. Goldstein, D. E. Newbury, D. C. Joy, C. E. Lyman, P. Echlin, E. Lifshin, L. C. Sawyer and J. R. Michael, *Scanning Electron Microscopy and X-Ray Microanalysis*, Plenum Press, New York, 3rd edn, 2003, pp. 5–10, ISBN: 0-306-47292-9.
- 36 D. B. Williams and C. B. Carter, *Transmission Electron Microscopy: A Textbook for Materials Science*, Plenum Press, New York, 4th edn, 1996, pp. 26–30, ISBN 0-306-45247-2.
- 37 S. S. Garje, J. S. Ritch, D. J. Eisler, M. Afzaal, P. O'Brien and T. Chivers, *J. Mater. Chem.*, 2006, **16**, 966.
- 38 S. S. Garje, D. J. Eisler, J. S. Ritch, M. Afzaal, P. O'Brien and T. Chivers, *J. Am. Chem. Soc.*, 2006, **128**, 3120.
- 39 W. Wang, B. Poudel, J. Yang, D. Z. Wang and Z. F. Ren, *J. Am. Chem. Soc.*, 2005, **127**, 13792.
- 40 S. S. Garje, M. C. Copesey, M. Afzaal, P. O'Brien and T. Chivers, *J. Mater. Chem.*, 2006, **16**, 4542.